J. Geogr. Sci. 2022, 32(10): 1935-1955
DOI: https://doi.org/10.1007/s11442-022-2030-5

Spatio-temporal correlation between human activity intensity and land surface temperature on the north slope of Tianshan Mountains

CHEN Hongjin[1,2], *LIU Lin[1,2], ZHANG Zhengyong[1,2], LIU Ya[1,2], TIAN Hao[1,2], KANG Ziwei[1,2], WANG Tongxia[1,2], ZHANG Xueying[1,2]

1. School of Science, Shihezi University, Shihezi 832000, Xinjiang, China;
2. Key Laboratory of Oasis Town and Mountain-basin System Ecology of Xinjiang Bingtuan, Shihezi 832003, Xinjiang, China

Abstract: Research on the spatio-temporal correlation between the intensity of human activities and the temperature of earth surfaces is of great significance in many aspects, including fully understanding the causes and mechanisms of climate change, actively adapting to climate change, pursuing rational development, and protecting the ecological environment. Taking the north slope of Tianshan Mountains, located in the arid area of northwestern China and extremely sensitive to climate change, as the research area, this study retrieves the surface temperature of the mountain based on MODIS data, while characterizing the intensity of human activities thereby data on the night light, population distribution and land use. The evolution characteristics of human activity intensity and surface temperature in the study area from 2000 to 2018 were analyzed, and the spatio-temporal correlation between them was further explored. It is found that: (1) The average human activity intensity (0.11) in the research area has kept relatively low since this century, and the overall trend has been slowly rising in a stepwise manner ($0.0024 \cdot a^{-1}$); in addition, the increase in human activity intensity has lagged behind that in construction land and population by 1–2 years. (2) The annual average surface temperature in the area is 7.18 ℃ with a pronounced growth. The rate of change ($0.02\ ℃ \cdot a^{-1}$) is about 2.33 times that of the world. The striking boost in spring ($0.068\ ℃ \cdot a^{-1}$) contributes the most to the overall warming trend. Spatially, the surface temperature is low in the south and high in the north, due to the prominent influence of the underlying surface characteristics, such as elevation and vegetation coverage. (3) The intensity of human activity and the surface temperature are remarkably positively correlated in the human activity areas there, showing a strong distribution in the east section and a weak one in the west section. The expression of its spatial differentiation and correlation is comprehensively affected by such factors as scopes of human activities, manifestations, and

Received: 2022-05-22 **Accepted:** 2022-07-10
Foundation: National Natural Science Foundation of China, No.41461086, No.41761108
Author: Chen Hongjin (1998–), Master Candidate, specialized in the research of human activity intensity and the human-land relationship. E-mail: ZLYZXLX@163.com
***Corresponding author:** Liu Lin (1981–), Associate Professor, specialized in the research of GIS application and remote sensing research of resources and environment. E-mail: liulin779@163.com
This paper is initially published in *Acta Geographica Sinica* (Chinese edition), 2022, 77(5): 1244–1259.

land-use changes. Vegetation-related human interventions, such as agriculture and forestry planting, urban greening, and afforestation, can effectively reduce the surface warming caused by human activities. This study not only puts forward new ideas to finely portray the intensity of human activities but also offers a scientific reference for regional human-land coordination and overall development.

Keywords: human activity intensity; surface temperature; nighttime light data; spatio-temporal correlation; north slope of Tianshan Mountains

1 Introduction

Activities of different scales and types in the process of human survival and development have had a sustained and far-reaching impact on all major Earth spheres, and their impact will be counterproductive to human self-welfare (Xu *et al*., 2015). The definition, quantification, and spatio-temporal expression of the intensity of human activities are one of the core research contents to evaluate the coupling relationship between human activities, ecosystems and climate change. The Fifth IPCC Climate Change Assessment Report explicitly indicated that human activities are the governing cause of global warming since the mid-20th century (Shen *et al*., 2013). The earth's surface is the principal direct heat source for the ground air. It is a vital scientific issue to analyze the process and mechanism of climate warming to comprehensively, objectively and subtly engrave human activities and their spatio-temporal relationship with the surface temperature.

Human Activity Intensity (HAI) is a comprehensive index that expresses the degree of disturbance of human activities in a specified area. It can objectively characterize the degree of utilization, transformation and development of the land surface by human activities (Xu *et al*., 2015), and its quantitative expression is an imperative parameter to evaluate the impact of human activities on the ecological environment (Liu *et al*., 2018). With the rapid development of the social economy and the tremendous changes in human production and lifestyles, the intensity, depth and scale of human transformation of nature are constantly expanding, and human activities tend to be diversified, complicated and integrated, which brings great challenges to objectively defining and characterizing the current intensity of human activities. In the past few years, the quantitative expression of HAI is mainly based on the results of human activities, such as weight-based multi-index overlay analysis (Duan *et al*., 2020), residual analysis (Yin *et al*., 2020), human footprint (Sanderson *et al*., 2002; Venter *et al*., 2016a; 2016b), land-use change (Xu *et al*., 2015; Han *et al*., 2017), etc. The selected indicators mainly include land use mode, landscape type and population density, etc. Most of them are single-factor quantification, failing to fully reflect the motivation and process of human activities, and the depiction of regional human activities is still rough and lopsided. Representative core indicators and their comprehensive quantitative analysis conduce to promote the comprehensive description and multi-dimensional expression of human activities. The population size and spatial distribution not only reflect the original power and basic pattern of human activities, but also reflect the dynamic evolution of the process, status and results of human activities; as the basic carrier of human activities, land-use change is an intuitive manifestation of the process and results of human impact on the surface, and it is currently one of the foremost factors in quantitatively characterizing HAI; night time light data can embody the low-intensity lights emitted by urban lights and even small-scale resi-

dential areas, traffic flow, etc. (He *et al*., 2006; Wang *et al*., 2012), so it can detail the level and spatial differentiation of human activities in industrial and mining land, transportation land, urban and rural housing and public facility land, and cultivated land, it has been extensively used in construction land extraction (Liu *et al*., 2012), urban development and spatial structure assessment (Ma *et al*., 2015), gross domestic product and energy consumption (Hu *et al*., 2018), carbon emission simulation (Foster, 1983), air pollution evaluation (Zhang *et al*., 2019) and other fields intimately connected to human activities over these years. At present, the comprehensive index algorithm with doughty universality and wide application has not yet been formed for the measurement of HAI (Xu *et al*., 2015) and a representation system that integrates land use, population distribution, and night light data is expected to further explain the initial dynamics, evolutionary process and spatio-temporal pattern of human activities, which is conducive to the overall characterization and multi-dimensional characterization of HAI and has imperative theoretical value and practical significance.

Land Surface Temperature (LST) is an indispensable parameter for global and regional land surface process and climate model research. It changes the material and energy balance between the ground and the atmosphere to cause a chain reaction of the spatio-temporal patterns of temperature, precipitation and vegetation, which in turn has a tremendous effect on the evolution of the regional ecological environment (Guan *et al*., 2015b). The research nowadays of land surface temperature based on remote sensing data has gained substantial achievements, of which MODIS ground temperature data has been widely used due to its economic convenience, macroscopic and high time resolution and many other advantages, and its accuracy has been universally recognized (Prihodko *et al*., 1997; Yang *et al*., 2015). Existing research chiefly focuses on the ground temperature changes (Christelle *et al*., 2009; Yang *et al*., 2015; Qiao *et al*., 2019), cold and heat island effects (Marc *et al*., 2010; Zhang *et al*., 2018) in densely populated areas such as central, eastern and southern China. Ground temperature is affected by many factors, and existing studies have shown that land-use types have a profound impact on the spatio-temporal distribution of LST (Reyilai *et al*., 2016; Lu *et al*., 2017), the LST of water-forest land-grassland-bare land-building land rises sequentially (Lu *et al*., 2017), NDVI and LST are generally negatively correlated (Lu *et al*., 2017; Guo *et al*., 2019). The concentration of population means more intense land surface transformation, further resource consumption and man-made heat emission, Guo *et al*. (2019) and Wang *et al*. (2019) confirmed the obviously positive impact of population density on LST; the intensity of nighttime light is a combination of land use and population factors, which directly embodies the social and economic activity, research by Shen *et al*. (2021) and Hu *et al*. (2021) found that its positive correlation with LST emerged a striking uptrend. It can be seen that existing studies are mostly single-factor correlation studies, while the multi-factor comprehensive linkage analysis is less, which cannot fully reveal the change mechanism of land surface temperature, nor reflect the comprehensive impact of human activities on LST. Therefore, the research on the impact of HAI on LST and its spatio-temporal differentiation urgently needs to be expanded and deepened.

The ecological environment in the arid region of Northwest China is fragile and sensitive to climate change, and its surface temperature has attracted great attention from all walks of life as an indicator of global climate change (Ouyang *et al*., 2012). For more than half a century, the overall trend of Northwest China is from warm dry to warm wet, especially in

northern Xinjiang and the Tianshan Mountains (Shi *et al*., 2002; 2003). As the core area of politics, economy and culture in Xinjiang, the north slope of Tianshan Mountains is the region with the densest population and the most active human activities (Guan *et al*., 2015a), relevant studies are mostly carried out separately from the perspectives of temperature, land-use change, and urbanization processes, etc. (Liu *et al*., 2020a; Qi *et al*., 2020), and the spatio-temporal relationship between regional human activities and the ground temperature remains to be expanded. Therefore, from the perspective of human activities' motivations and results, status and processes, this study attempts to construct a comprehensive HAI indicator that can accurately and objectively reflect the impact and effect degree of human activities on the land surface by organically integrating the data of land use, nighttime light and population distribution. Utilizing slope analysis and correlation analysis, the spatio-temporal differentiation characteristics, trends and relevance between human activity intensity and surface temperature on the north slope of Tianshan Mountains were quantitatively studied, and evaluate the impact of HAI on LST changes on the north slope of Tianshan Mountains, hoping to be positive provide a reference for responding to climate change, protecting the ecological environment, rationally developing resources and regulating human activities, etc.

2 Data and methods

2.1 Study area

The north slope of Tianshan Mountains, lying between 42°55'N–46°13'N and 83°25'E–88°58'E, is located in the northern part of the middle Tianshan Mountains and the southern margin of the Junggar Basin. It is adjacent to the Tianshan Mountains area to the south and the Gurbantunggut Desert to the north. The alluvial flat central principle distributes the broad oasis agricultural area and 11 counties and cities (Figure 1). The study area is under a typical temperate continental climate. The terrain is high in the southeast and low in the northwest, and the landscape types from south to north are the medium-alpine mountain belt, foreland mountain belt, oasis, oasis-desert transitional zone and the desert (Luo *et al*., 2003). There are obvious interactive responses between vegetation cover types and climate change (Sun *et al*., 2014). Due to the central alluvial plain being suitable for agricultural development, especially since the 21st century, the cultivated land area has been continuously increasing and the urbanization degree has been continuously enhanced, the north slope of Tianshan Mountains has become one of the most conspicuous areas affected by human activities in Xinjiang (Yin *et al*., 2020).

2.2 Data sources

The data used in this article mainly include MOD11C3 ground temperature data, Land Use (LU) data, Normalized Differential Vegetation Index (NDVI) data, DMSP/OLS and NPP-VIIRS nighttime light (NTL) Data and Population Distribution (PD) data, etc. (Table 1). MOD11C3 was utilized to explore the characteristics of spatio-temporal differentiation of ground temperature. LU, NTL and PD data were applied to characterize HAI and analyze its spatio-temporal distribution characteristics. NDVI data incarnate the changes in vegetation

coverage on the underlying surface.

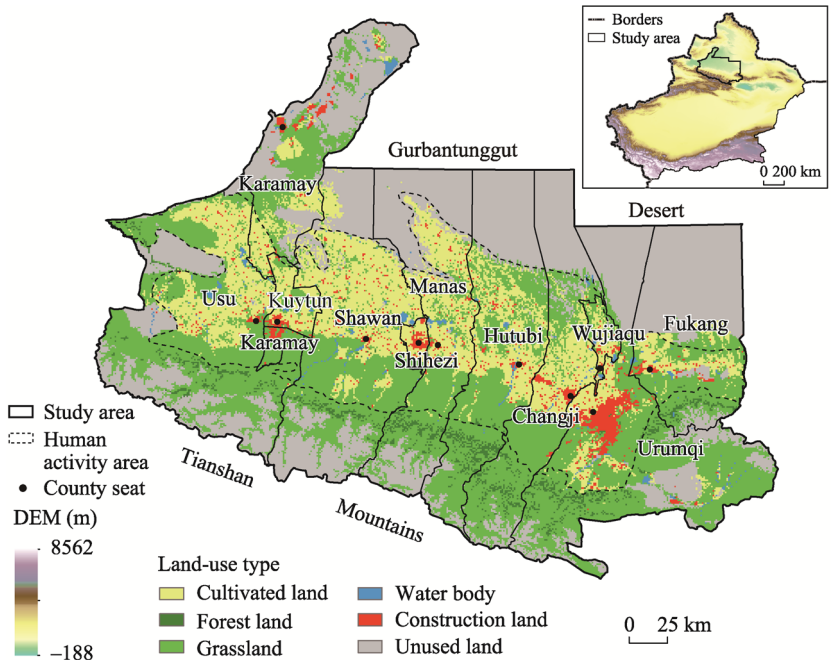

Figure 1 Overview of the study area (north slope of Tianshan Mountains)

Table 1 Data sources

Data	Spatial Resolution	Time	Sources
MOD11C3	0.05°×0.05°	2000–2019	ladsweb.nascom.nasa.gov/data/search
LU	1 km×1 km	2005, 2010, 2015, 2018	http://www.resdc.cn/Default.aspx
NDVI	1 km×1 km	2000–2018	http://www.resdc.cn/Default.aspx
DMSP/OLS	1 km×1 km	2000–2013	http://www.resdc.cn/Default.aspx
NPP-VIIRS	500 m×500 m	2014–2018	https://ngdc.noaa.gov/eog/dmsp/downloadV4composites.html
PD	1 km×1 km	2000–2018	https://landscan.ornl.gov/landscan-datasets

2.3 Methods

2.3.1 Data preprocessing

For the sake of facilitating grid calculation and statistical analysis, all data adopt the WGS-84 coordinate system and UTM projection. At the same time, MOD11C3 and NPP-VIIRS data are resampled to 1 km×1 km to unify the spatial resolution.

(1) MOD11C3: The batch processing function of MRT software was applied to carry out geometric correction and re-projection, and the mosaic and cropping were carried out in ArcGIS10.3, utilizing a raster calculator to convert K temperature to Celsius temperature.

(2) NTL: (i) Desaturation treatment: Due to the low radiation resolution of the sensor, DMSP/OLS data has a large number of saturated pixels with brightness values in the central area of the city, which makes the brightness levels indistinguishable and requires desaturation processing. Previous studies have proved (Pan *et al*., 2016) that the values of NDVI and

DMSP/OLS are negatively correlated, so NDVI data are introduced in this paper. The DMSP/OLS normalized NTL data were desaturated by three desaturation index models: Ratio Nighttime-light Vegetation Index (RNVI), Normalized Difference Nighttime-light Vegetation Index (NDNVI) and Modified Difference Nighttime-light Vegetation Index (MDNVI). The results obtained after comparison are similar to Pan *et al.* in desaturation of night light data, the MDNVI was more detailed in describing the actual difference degree inside the nighttime light, and the processing effect on the saturated area of image gray value was the most prominent (Figure 2). Therefore, this paper adopted the MDNVI model to de-saturate DMSP/OLS data from 2000 to 2013. (ii) DMSP/OLS and NPP-VIIRS integration: By reason of the differentiation in sensor parameters, sensitivity levels and spectral response modes, the gray values of the two types of images are quite different in magnitude, and cannot be used directly at the same time. Referred to the data integration method of Li *et al*. (2017) and Yang *et al*. (2018), this study selected the image of 2013 in the coincident year as the sample data, took the obvious correlation between the two types of data as the benchmark, and used NPP-VIIRS data to fit the DMSP/OLS data of the corresponding year. The obtained fitting formula was applied to NPP-VIIRS data from 2014 to 2018 to complete the integration of DMSP/OLS and NPP-VIIRS data.

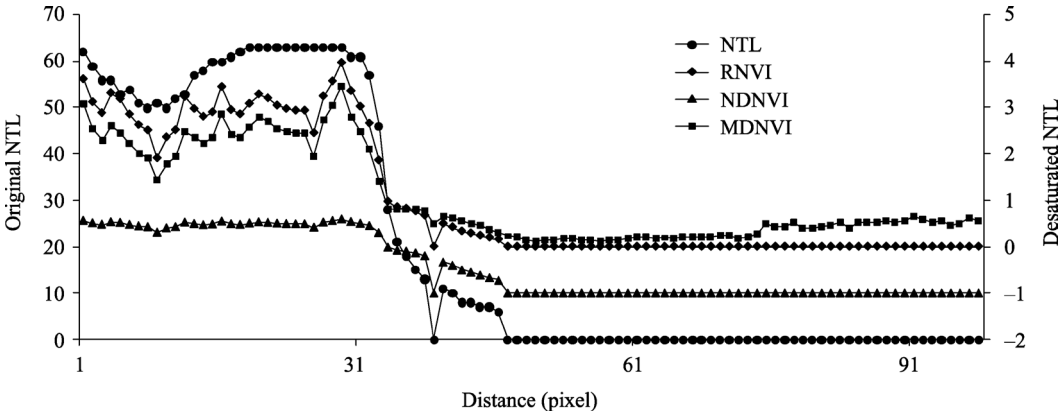

Figure 2 Comparison of night light brightness value and saturation index value of the zonal transect on the north slope of Tianshan Mountains in 2010

2.3.2 Representation of human activity index

The intensity of human activities represents the impact of human activities on the land surface, and "Utilization, transformation and development of the land surface by humans" can be regarded as the principal part of human activities (Xu *et al*., 2016), but not all. The single data of land use is difficult to represent the diversity, complexity and comprehensiveness of human activities. Based on the basic framework of land use data, supplemented by the data of population distribution and nighttime light, this paper concentrated on the dynamic description of the whole process, status and results of human activities, and takes into account the multi-scale description of the macroscopic distribution pattern of human activities and the micro-hierarchical difference, and constructs the HAI representation model:

$$HAI=aN+bP+cL \quad (1)$$

where *HAI* is the intensity of human activities; *N*, *P*, and *L* respectively represent the nor-

malized night light brightness, population and land use data; *a*, *b*, and *c* are the weights of NTL, PD, and LU respectively.

The weights of a, b and c were rated as 0.3, 0.3 and 0.4 by more than 40 experts on the Likert 5-point scale. The results were tested by Kendall coordination coefficient, p=0.000, which indicated that the scores were significantly consistent and the results were reliable. The weight of each category of LU (Table 2) was determined by AHP analytic hierarchy process after comprehensive reference to related pieces of literature (Zhang *et al*., 2004; Wang *et al*., 2020), and participated in the calculation of HAI after normalization. The value of HAI is between 0 and 1, and the higher the value is, the stronger the human activity. According to HAI=0, $0<\mathrm{HAI}\leqslant 0.2$, $0.2<\mathrm{HAI}\leqslant 0.4$, $0.4<\mathrm{HAI}\leqslant 0.6$, $0.6<\mathrm{HAI}\leqslant 0.8$ and $0.8<\mathrm{HAI}\leqslant 1$ (Wang *et al*., 2020) divides human activities into six intensity levels: extremely low, low, medium-low, medium, medium-high and high.

Table 2 Weight of land-use type

Land-use type	Cultivated land	Forest land	Grassland	Water body	Construction land	Unused land
Weights	0.30	0.05	0.05	0.05	0.55	0.00

2.3.3 Slope analysis

The slope analysis method can simulate different grid change trends (Wei *et al*., 2007) to analyze the spatial change characteristics of the surface temperature and the intensity of human activities in different periods. The formula (Guan *et al*., 2015a) is as follows:

$$\theta=\frac{\sum_{i=1}^{n}a_ib_i-\frac{1}{n}\sum_{i=1}^{n}a_i\sum_{i=1}^{n}b_i}{\sum_{i=1}^{n}b_i^2-\frac{1}{n}\left(\sum_{i=1}^{n}b_i\right)^2} \tag{2}$$

where θ is the interannual rate of change; n is the number of years, which is used in this article as 20; b_i is the time series value, which is 1–20 in turn from 2000 to 2019; a_i is the LST/HAI value of the ith year. $\theta<0$ and $\theta>0$ respectively indicate that HAI and LST decrease and increase with time; the larger the absolute value of θ, the faster the change of HAI and LST.

2.3.4 Correlation coefficient method

Correlation analysis is a statistical method to analyze the closeness of variables. By calculating the correlation coefficient between the average annual HAI and LST, it can effectively reflect the closeness of the correlation between the variables. The value range of the correlation coefficient R is [–1, 1], the formula is as follows:

$$R=\frac{\sum_{i=1}^{n}x_iy_i-\frac{1}{n}\left(\sum_{i=1}^{n}x_i\right)\left(\sum_{i=1}^{n}y_i\right)}{\sqrt{\sum_{i=1}^{n}x_i^2-\frac{1}{n}\left(\sum_{i=1}^{n}x_i\right)^2}\times\sqrt{\sum_{i=1}^{n}y_i^2-\frac{1}{n}\left(\sum_{i=1}^{n}y_i\right)^2}} \tag{3}$$

where R is the correlation coefficient; n is the number of years, ranging from 1 to 20; x_i is

the normalized surface temperature, and y_i is the intensity of human activities. And $R<0$ and $R>0$ respectively indicate that HAI and LST are negatively correlated and positively correlated; the correlation reinforces the upswing of the absolute value of R. The correlation coefficient is divided into six levels: strong negative correlation ($-1 \leqslant R \leqslant -0.6$), moderately strong negative correlation ($-0.6 < R \leqslant -0.3$), weak negative correlation ($-0.3 < R \leqslant 0$), weak positive correlation ($0 < R \leqslant 0.3$), moderately strong positive correlation ($0.3 < R \leqslant 0.6$), and strong positive correlation ($0.6 < R \leqslant 1$).

3 Results

3.1 Spatio-temporal characteristics of HAI on the north slope of Tianshan Mountains

From 2000 to 2018, the intensity of human activities in the north slope of Tianshan Mountains was low and showed a gradual upward trend, with an average annual HAI of 0.11 and a rate of change of $0.0024 \cdot a^{-1}$ (Figure 2). Between 2001–2003, the population of the study area grew slightly, while the construction land and cultivated land area were in the expansion stage. Under the joint influence of the three factors, the HAI in the study area showed a slight increase, and then entered a platform period lasting nearly 10 years. Then, the population grew rapidly from 2012 to 2015, and the expansion of the construction land and cultivated land area resulted in significant aggrandizement in HAI. It can be seen that HAI is predominantly affected by population and construction land, with a lag period of 1–2 years, while the impact of other land types is relatively small (Figure 3b), which also incarnates the one-sidedness of use LU only in characterizing HAI and the rationality of PD in explaining HAI changes.

The spatial differentiation of HAI in the study area is high in the middle and low in the north and south (Figure 4a). The southern mountainous area, northern desert area and low-mountain steppe zone are areas with low human activity and extremely low intensity, accounting for 76.2% of the total area. The cultivated land is predominantly medium-low intensity, and the high-intensity and medium-high intensity areas are concentrated in the urban center as the HAI in Urumqi, Shihezi and Karamay are all above 0.73. From the perspective of spatial distribution, the spatial distribution of HAI in counties and cities con-

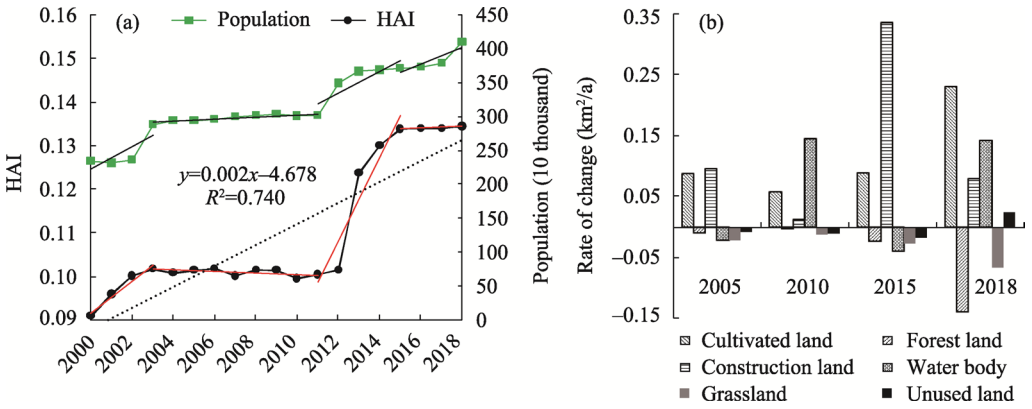

Figure 3 Annual average HAI and population changes (a) and area change rate of various land-use types (b) on the north slope of Tianshan Mountains, 2000–2018

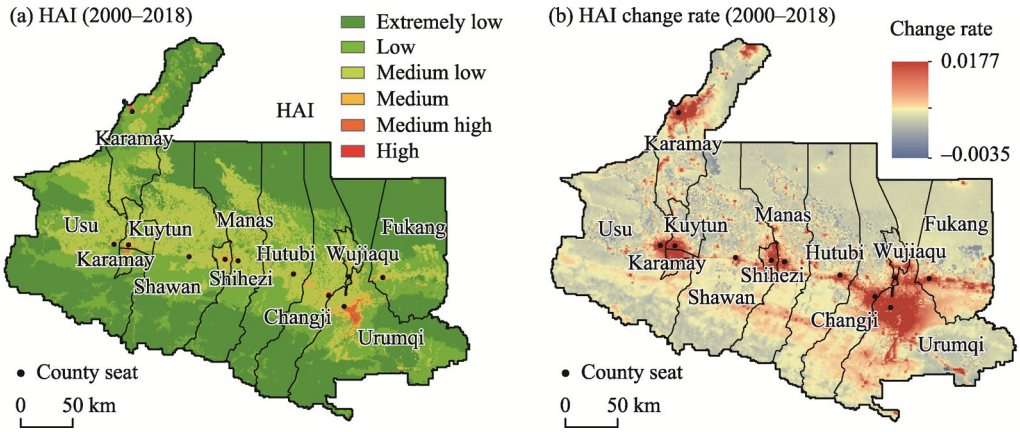

Figure 4 Spatial distribution of the intensity (a) and change rate (b) of human activity on the north slope of Tianshan Mountains, 2000–2018

forms to the circle structure characteristics of urban development (Figure 4b), which shows that HAI and its change rate gradually attenuate from the central city to the outer edge of the city and the surrounding cultivated land, grassland and desert, with Urumqi as the most typical. However, the high-value areas of HAI variability outside the central urban area are all rural residential areas scattered in cultivated land. Judging from the interannual variation of the area proportion of HAI levels, the area proportion of extremely-low intensity levels (unused land) of human activities has dropped significantly from 49.48% in 2000 to 6.93% in 2018, and the areas of the remaining levels are escalating, with the medium-low intensity level (primarily cultivated land, accounting for 41.96%) being the most pronounced. It serves to show that the scope of human activities in the study area is constantly expanding and the scope of radiation influence on the surrounding areas is continually enhancing, and the variation of HAI follows the law of distance attenuation.

From 2000 to 2018, the HAI on the north slope of Tianshan Mountains has been relatively low, with an annual change rate of only $0.0024 \cdot a^{-1}$, showing a slight and slow growth trend. Compared with previous research results based on different scales, the growth rate is very small, such as $0.038 \cdot a^{-1}$ in the country (Xu *et al*., 2016) and $0.061 \cdot a^{-1}$ in Hainan province (Liu *et al*., 2020b), which reflects from the side that the relatively lagging socio-economic development and the slow growth of the study area are due to the historical reasons and restrictions on location, geography, etc. The positive growth area of HAI in the study area accounts for 99.33%, and it is rapidly attenuating from the central urban area to the periphery. HAI around scattered rural settlements increased obviously, while other land types have not changed much, which is chiefly due to the centralization of population, the augment of urban-industrial investment (Zhong *et al*., 2008), the expansion of residential buildings, industrial and mining land and road construction (Figure 3b), and the continuous transformation of marginal land to construction land (Figures 1 and 4b), which embodies the expansion and development trend of urban scale.

3.2 Spatio-temporal characteristics of LST on the north slope of Tianshan Mountains

During the study period, the annual average LST of the north slope of Tianshan Mountains was 7.18℃, and the coldest and hottest years were 2003 (6.03℃) and 2015 (8.21℃) respec-

tively. The four seasons of LST in 2006 and 2008 were all higher than the multi-year average. Compared with 2000, the LST in the study area increased by 0.82 ℃ in 2019, with an average annual change rate of 0.02 ℃·a^{-1}, showing a salient fluctuating upward trend (Figure 5a) and was much stronger than the global warming (0.0086±0.006 ℃·a^{-1}) (Yun, 2019). The spring, summer, and winter have shown a warming trend in the past 20 years, with positive anomaly years being the majority. The significant warming in spring (0.068 ℃·a^{-1}) made an absolute contribution to the overall warming of the study area (Figure 5a). However, the negative anomaly of LST in spring was larger, and extremely low temperatures occurred frequently in many areas (Mao *et al*., 2016). LST was relatively stable in summer but fluctuated greatly in winter, and the warming in winter showed an upswing trend over the years.

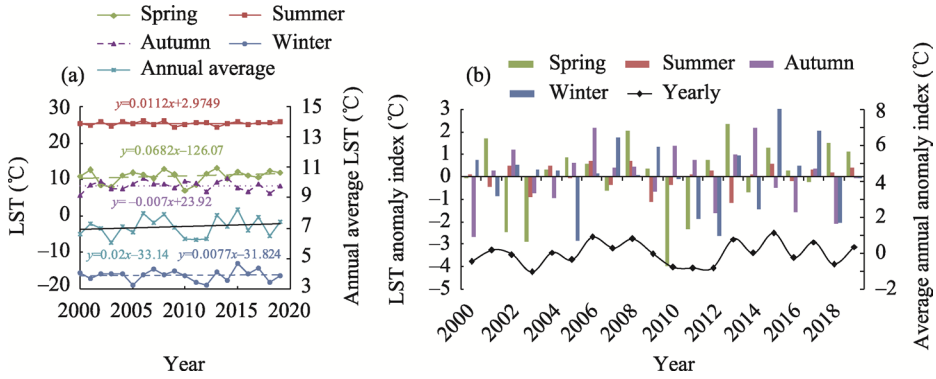

Figure 5 Average surface temperature, seasonal variation and surface temperature anomaly index on the north slope of Tianshan Mountains, 2000–2019

The LST in the study area was lower in the south and higher in the north, with prominent spatial differentiation. According to the LST statistics of the longitudinal in the central part of the study area (Figure 6b), the LST in the southern mountainous area decreased conspicuously with the increase in altitude, and the correlation coefficient reached –0.84, showing a significant negative correlation, which intuitively reflected the vertical zonality of LST. The LST in the strip-shaped urban area in the piedmont alluvial plain is signally higher than that of the natural vegetation and arable land on both sides, up to 15.23 ℃, and there is an obvious "heat island effect", mainly due to the artificial heat emission from industry, traffic and life, the physical characteristics of small specific heat capacity, high heat storage and low loss of urban impervious surface, as well as the "insulation" effect of air pollutants. The desert area on the southern margin of the Junggar Basin has a relatively high LST due to its own small specific heat capacity and lack of vegetation evapotranspiration, humidification, and shading. It serves to show that the elevation and underlying surface break the gradual warming characteristic of LST in the study area from south to north along the latitudinal direction, and human activities, as a momentous "force", play a crucial role in the process of ground temperature change by changing land-use patterns.

LST on the north slope of Tianshan Mountains increased greatly in the past 20 years, and the rate of change was also low in the south and high in the north, with pronounced spatial differences (Figure 6c). The area of the heating zone is about 4.6 times that of the cooling zone, and the desert areas with bare surfaces and sparse vegetation, as well as the urban and

surrounding areas predominantly showed warming. The desert area on the southern margin of the Junggar Basin is the region with the most conspicuous warming, with a change rate of as high as 0.09 ℃·a^{-1}. The densely populated urban and rural construction land is mostly impervious surface. Due to its higher heat absorption rate and smaller specific heat capacity, the surface heats up rapidly, combined with the thermal insulation effect of production and domestic waste heat emissions and air pollutants, it has become a regional heat island and the dominant temperature rise Area. For example, the surrounding countries and cities of Urumqi, the central urban areas of Hutubi and Manas-Shihezi present obvious hot areas, and the range of LST changes in some areas exceed 0.1℃·a^{-1}. However, there is a conspicuous cold zone in the Kuytun-Usu area, the statistics found that the NDVI of Kuytun City has risen from 0.29 to 0.62, and a good deal of natural grasslands in the city have been converted into cultivated land. Although it was still vegetation under the manual intervention of wasteland reclamation and agricultural planting, the growth was more vigorous and the coverage increased substantially. The accompanying decrease in surface albedo and increase in soil moisture should be one of the reasons for the cooling of the area, which also confirms that the changes in the physical and biological properties of the underlying surface caused by vegetation coverage and human activities are intimately connected to the changes of LST. It is particularly noteworthy that some high-altitude mountains in the south of Usu and Fukang city present obvious warming trends, and the rise of LST will aggravate the melting of glaciers. Meanwhile, the increase of surrounding bare rock, the aggravation of heat absorption and the reduction of the reflectivity of the underlying surface will lead to the rise of LST (Huang *et al*., 2016). Just as Wang *et al*. (2017) concluded that the change rate of glacial reserves in Glacier No.1 at the head of the Urumqi River was as high as –291.82 mm·a^{-1} from 1959 to 2010, which is a shred of good evidence for the conspicuous rise of LST in the region. The mounting risk of accelerated glacier

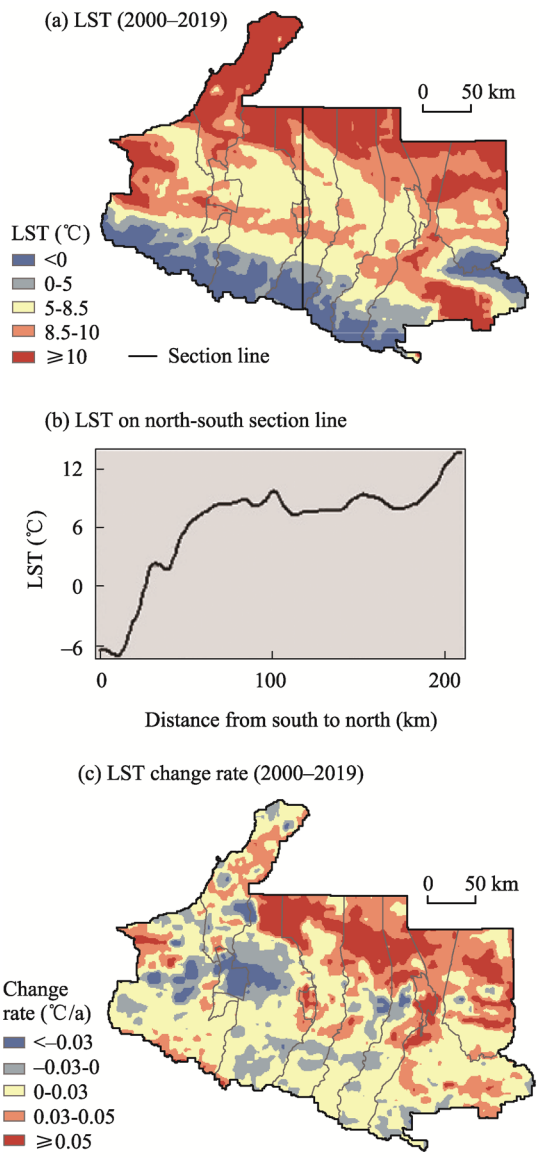

Figure 6 Average annual surface temperature (a) and inter-annual rate of change (b) on the north slope of Tianshan Mountains, 2000–2019

melting will have a profound impact on the ecological environment, industrial and agricultural development and social economy in the study area (Zhang *et al*., 2019).

3.3 Spatio-temporal correlation analysis of HAI and LST

This article centralized the principal human activity areas in the central part of the study area (Figure 1) to explore the spatio-temporal relationship between HAI and LST, as the southern mountainous and northern desert areas are inaccessible. Spatial correlation analysis showed that HAI and LST were significantly positively correlated, showing a strong distribution in the east and a weak in the west (Figure 7). The area of positive correlation accounted for 94.6%, primarily cultivated land and construction land, of which 73.7% was a moderately strong and strong positive correlation, with Urumqi (0.78) and Wujiaqu (0.84) being the most prominent. The HAI in Fukang City and the central part of Changji City was noteworthily enhanced (Figure 4), appearing a strong positive correlation. HAI and LST generally show a strong positive correlation in the central and northern regions due to the combined effects of the large increase of cultivated land, the expansion of internal rural settlements, and the substantial upswing of urban construction land in the center of each county, and the increase of NTL. However, in areas with a strong positive correlation, except for the extension of unused land in the north of Changji and the small expansion of rural settlements in Wujiaqu, the other land-use types did not get marked variation (Figure 7b). The increase in LST should be positively correlated with the slight growth in population (Figure 7c) and the enhancement in NTL brightness (Figure 7d). In the south large grassland area, the population

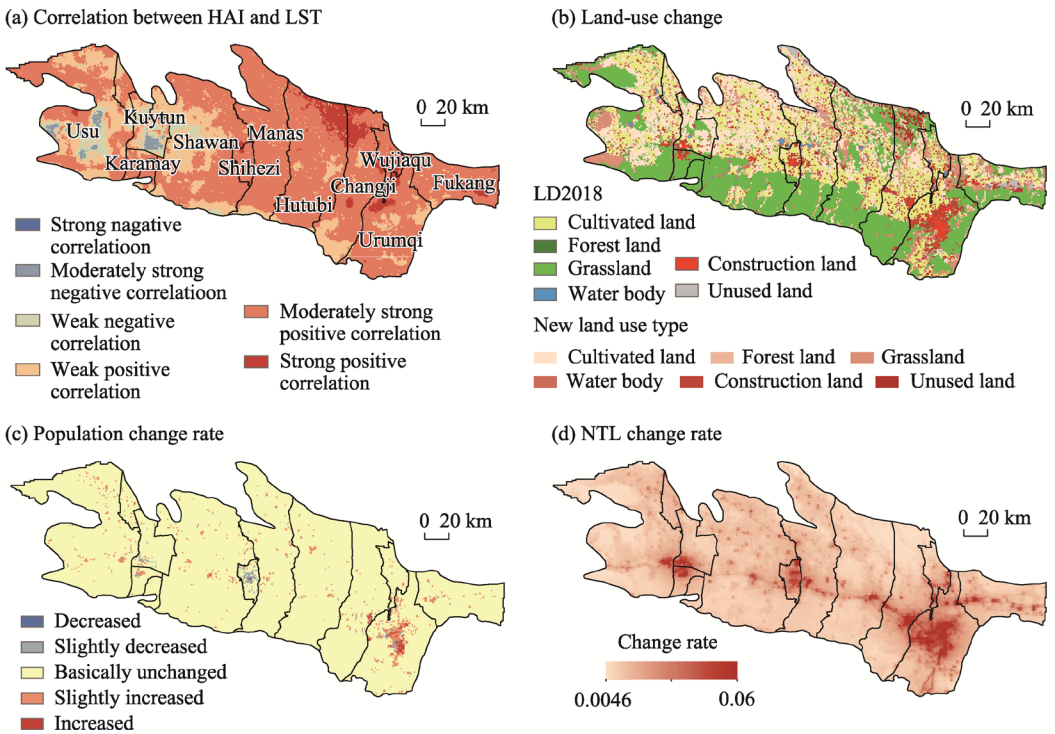

Figure 7 The correlation coefficients between surface temperature and human activity intensity (a), land-use change (b), population(c) and NTL (d) change rate on the north slope of Tianshan Mountains, 2000–2018

has not changed much over the years, but the area of internal cultivated land and rural settlements around water body has expanded, NTL has generally enhanced, and HAI and LST are also positively correlated. In addition, cultivated land expanded obviously in the south of Urumqi, the rural residential area and urban construction land increased, the population and NTL also augmented greatly, and the correlation between HAI and LST showed a strengthening trend.

There are few areas with a negative correlation between HAI and LST, which are only located in small areas of cultivated land and grassland around Usu and Kuytun. Under the condition of slight enhancement of HAI, LST declines prominently, presenting a conspicuous negative correlation (Figure 7). Combined with the manifestations of human activities in different land-use types, the comparison found that NDVI in this region has been continuously escalating over the years, and the cooling effect of vegetation is the dominant factor leading to its negative correlation. Take Kuytun City as an example (Figure 8), 42.78% of the sparse grassland area has been transformed into cultivated land with higher coverage (Figures 8e and 8f) for nearly 20 years, although the land type has changed, it has only changed from natural vegetation to artificial vegetation, its essence has not changed. Moreover, the NTL intensity is slightly enhanced when the population is basically unchanged, so the area HAI is only slightly increased. The NDVI of the region escalated from 0.30 to 0.62 (Figures 8g and 8h), the LST reduced by 4.66 ℃, and the NDVI (0.73) of cultivated land was 0.25 higher than that of grassland in the same year, while the LST was 0.48 ℃ lower than that of grassland. It serves to show that the shading, heat absorption and humidification effects of corps have gradually become prominent, thus saliently reducing LST. In general, human activities based on land reclamation and agricultural planting make crops under artificial control grow more vigorously and have higher coverage than natural vegetation, and cooperating with agricultural activities such as irrigation has intensified the cooling effect. By analogy, human greening and maintenance activities associated with vegetation, such as agriculture and forestry planting and cultivation, urban greening and afforestation, can pronouncedly inhibit the rise of LST.

In conclusion, the HAI and LST in the human activity area on the north slope of the Tianshan Mountains are strikingly correlated and show an escalating trend. Their spatial differentiation is comprehensively affected by the human activity ranges, manifestations, land-use changes and other factors, of which human activities lead to changes in underlying surface properties such as the continuous growth of population, the expansion of construction land to cultivated land, grassland and reclamation are the principal reasons for LST changes in the study area, and the change of PD and NTL can support a rational explanation of LST's spatio-temporal changes.

4 Discussion

4.1 Human activity intensity and characterization methods

For the definition and characterization of HAI, currently, it is mostly based on the single factor of land use (Xu *et al*., 2016; Han *et al*., 2017; Li *et al*., 2018) or combined with regional economic data, landscape types, population density and other data (Liu *et al*., 2018).

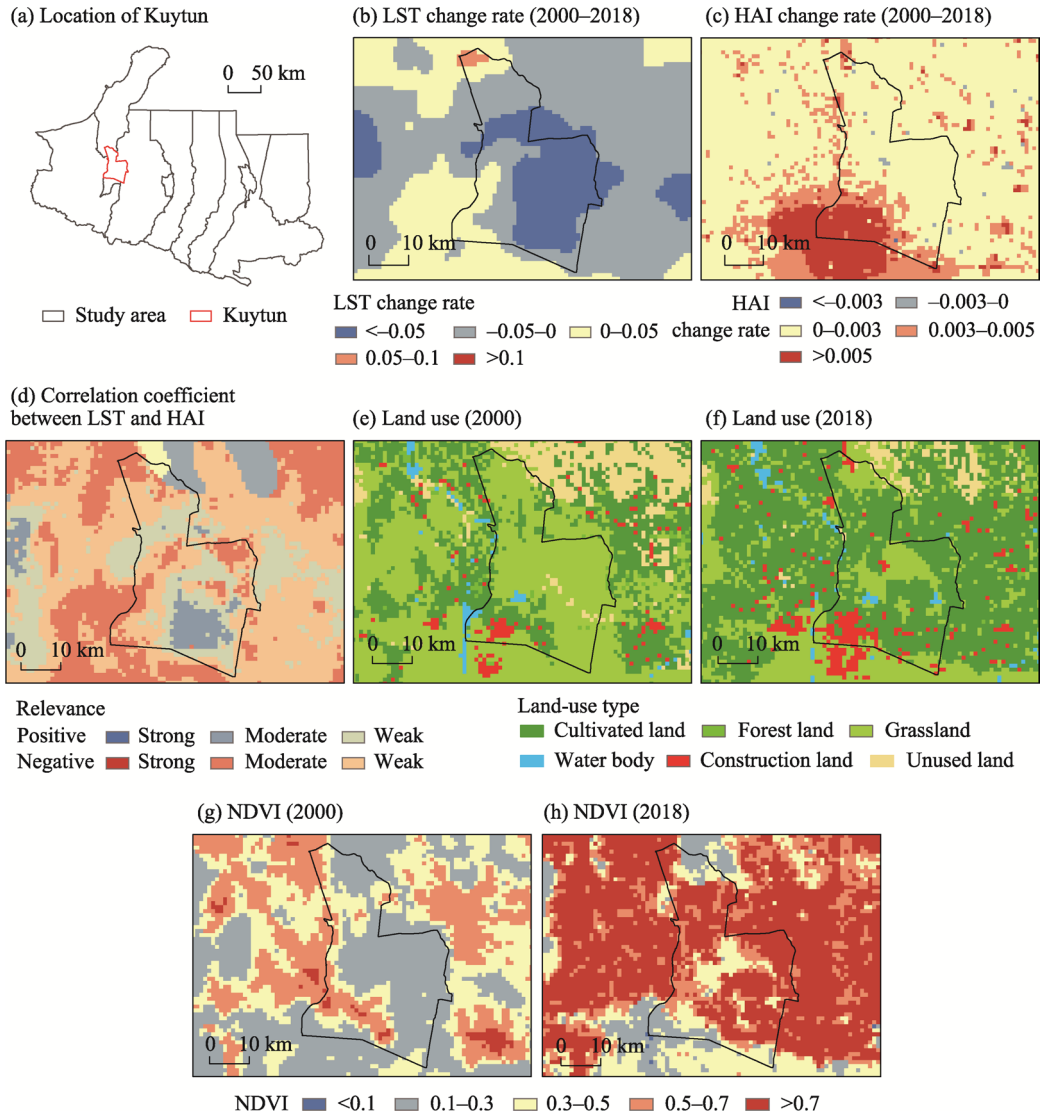

Figure 8 LST, HAI, land use, NDVI and their changes in Kuytun, 2000–2018

Scholars such as Liu *et al*. (2020b) and Xu *et al*. (2016) proposed the method of the equivalent factor of construction land area to represent HAI; Han *et al*. (2017) calculated HAI comprehensively based on the influence and weight of different land-use types; Rong *et al*. (2017) obtained HAI through the artificial influence parameters of regional landscape types; Xue (2021) reflected the change of HAI with population density. Whether the changes in land-use type/landscape type or population density can only incarnate a certain part of the influence of human activities and cannot reveal the panoramic image of human activities. Among the many existing HAI studies, the multi-stage data set of human activity intensity in the Yangtze River Economic Belt (Li *et al*., 2018) developed on the basis of China's national-scale land use data is represented by adopting the comprehensive evaluation scheme of ecosystem human disturbance index (hereinafter referred to as the comprehensive evaluation scheme). To compare the rationality and applicability of different schemes, the HAI of the

north slope of Tianshan Mountains was calculated according to the comprehensive evaluation scheme and normalized separately with the results of this study (Figure 9). The area of grassland (39.8%), unused land (33.7%) and cultivated land (20.7%) in the study area are much larger than the construction land (2.5%). Through comparative analysis, impute to the intense influence of the area proportion of each land-use type on the comprehensive evaluation scheme (Zhao *et al*., 2015), under the condition that the assignment level of each category is certain, cultivated land and grassland areas with a low level of assignment but a large area have a high HAI and low discrimination (Figure 9b), while the HAI for construction land with the most concentrated and intense human activities is low. While the results of this paper can not only reflect the macroscopic distribution pattern of HAI but also refine the spatial differences of HAI within different land types. As the author of the data set said, "The comprehensive evaluation scheme fails to fully reflect the multi-faceted disturbance of the ecosystem by humans, and is a conservative estimate of HAI" (Li *et al*., 2018). It is extremely widespread in arid, semi-arid areas and vast underdeveloped areas that the territory is vast and sparsely populated and the area of construction land is relatively small. In contrast, this study combined LU data with PD data and NTL data to consider the dynamics, status, process and results of ecological environment disturbance more thoroughly. The results in towns and surrounding areas were more objective, and the comparison of the disturbance degree of human activities among different land types was more reasonable. Therefore, the HAI representation system constructed in this study is relatively more universal.

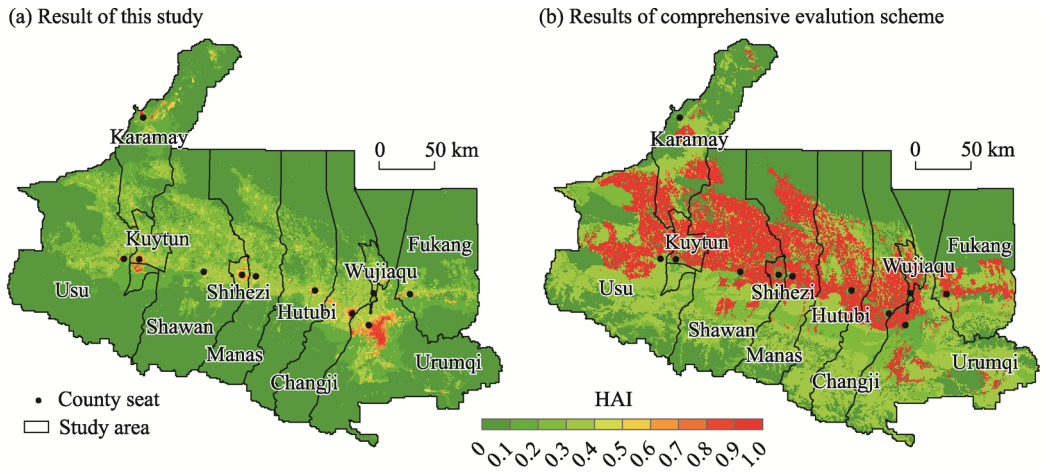

Figure 9 Comparison of different representations of human activity intensity on the north slope of Tianshan Mountains in 2018

At present, the characterization of HAI by NTL data is still in the preliminary stage of exploration, although many scholars have constructive comments and expectations on it (Wang *et al*., 2012; Deng *et al*., 2018). Scholars such as Duan *et al.* (2020), Sanderson *et al.* (2002) and Venter *et al.* (2016b) have introduced NTL data into the study of human activity intensity, but most of them only use DMSP/OLS data. The characterized human activity intensity has time discontinuity and data inefficiency, which cannot reflect the current situation and continuous change trend of regional human activity intensity, due to the absence of

DMSP/OLS data after 2013. This article attempts to combine the continuous NTL data, PD data and LU data to characterize HAI, which can be used as a reference and useful supplement for the characterization of human activity intensity in the future. Of course, methods to better characterize the intensity of human activity based on NTL data need to be explored in future research.

4.2 The impact of human activities on the LST

The results of this study indicated that HAI and LST were positively correlated in the human activity area on the north slope of Tianshan Mountains and had an escalating trend, and the changes in land use, population distribution and nighttime light could support a rational explanation for the spatio-temporal changes of LST, which was consistent with the previous conclusions (Wang, 2008; Deng *et al*., 2018; Chu, 2019), and human activities did have a pronounced impact on LST. However, the types and manifestations of human activities are diverse, and their effects on LST are also different. As the most intuitive embodiment of human activities, land use patterns can be used to explore the effects of different types of human activities on LST.

The spatial partition statistical method was used to quantitatively analyze the LST changes in the land-use change areas of human activity areas in each stage (Figure 10). This article only counts the six types of transformation with the largest area, on account of the complexity of land class conversion, and the large uncertainty of LST change that exists in the converted land class with a small area. When human activities manifest as the expansion of construction land, the increase of the impervious surface area of construction land converted from cultivated land and grassland leads to the enhancement of the heat island effect (Dong, 2012; Zeng, 2015), and the average temperature rise of LST is the highest in the first stage, reaching $0.36℃·5a^{-1}$. The phenomenon of cooling ($–0.11℃·5a^{-1}$) in the area converted to construction land in the second stage is caused by the conversion of large areas of deserts, bare land and other unused lands to construction land. Hence one can see that the transformation of different land types by human beings will have different effects on the LST for the expansion of construction land. When human activities manifest as vegetation destruction (Cui *et al*., 1998), resulting in the increase of secondary unused land, vegetation degradation, etc., natural vegetation such as forest and grassland is destroyed, and the land is abandoned

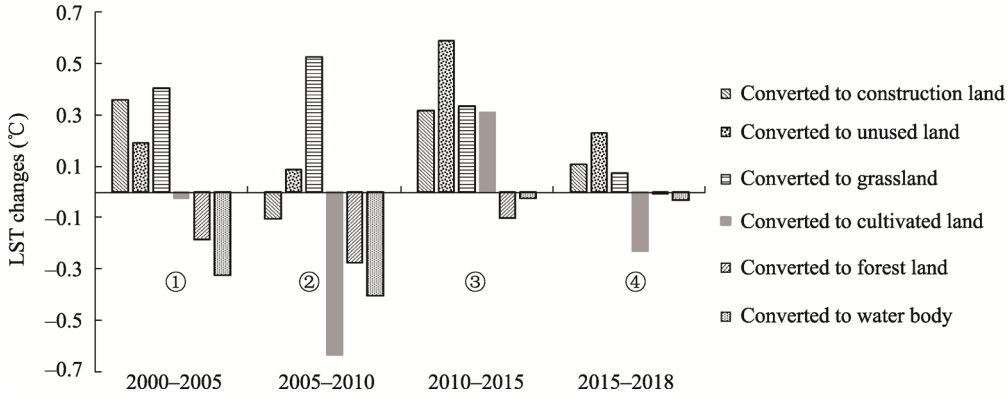

Figure 10 Surface temperature change in land use type conversion area

and converted to sparse grassland or even unused land so that the conversion to unused land and grassland areas generally present a warming state. The newly-added unused land in the study area is primarily distributed in the northern desert area, and the loss of bare surface water content and specific heat capacity due to vegetation degradation and land abandonment leads to an average LST warming of 0.27 ℃·5a^{-1}. The most significant warming is in the third stage (0.58 ℃·5a^{-1}), which is 13.49 times the global warming. When human activities manifested as wasteland reclamation and vegetation restoration, the accompanying reduction in deserts and bare land and the growth in vegetation coverage have a conspicuous cooling effect (Xia *et al*., 2010; Lu *et al*., 2017). The LST of newly added cultivated land and forest land in this area was cut down by 0.15 ℃·5a^{-1} and 0.14 ℃·5a^{-1} respectively, attribute to the increase of vegetation coverage and moisture content. The new water area is cooled due to a larger specific heat capacity and has a better regional temperature regulation ability. In the regions where the land type remains the same, the LST also showed an upswing trend, and the temperature in the construction land was the most prominent. The maximum impact of population on LST was 0.005 ℃·5a^{-1}·thousand people^{-1}, and the LST rose by 0.18 ℃ at most with the upswing of normalized NTL intensity by 0.01. When the population size and density grow and the brightness of nighttime lights upswing, it means that the intensity of land development and utilization aggrandizes, the social and economic activity upgrades, and the intensification level of human production and living and energy consumption elevates, which directly leads to the salient rise of LST (Guo *et al*., 2019; Wang *et al*., 2019; Hu *et al*., 2021; Shen *et al*., 2021). Certainly, the types and manifestations of human activities have anisotropic and cross-permeable effects on LST, and the quantification of the effects of different scales and forms of human activities on LST needs to be further explored in prospective research.

5 Conclusions and prospects

Characterize the human activity intensity index based on nighttime light, population distribution, and land use data, and conduct a multi-scale analysis of the spatio-temporal differentiation characteristics and spatial correlation of HAI and LST on the north slope of Tianshan Mountains from 2000 to 2018. The main conclusions are as follows:

(1) The intensity of human activities on the north slope of Tianshan Mountains was relatively low, with an average annual HAI of 0.11. The overall trend of gradual and slow increase (0.0024·a^{-1}), is primarily affected by the increase in construction land and population with a 1–2 years lag period. HAI was high in the middle and low in the north and south, and gradually diminished from the urban central belt to the periphery cultivated land, grassland, desert and mountainous area. HAI showed a slight slow growth trend from 2000 to 2018. The area of extremely low intensity minified dramatically, while the area of medium-low intensity expanded pronouncedly.

(2) The LST on the north slope of the Tianshan Mountains rose significantly and rapidly with an annual average LST of 7.18 ℃ from 2000 to 2019. The change rate (0.02 ℃·a^{-1}) was about 2.33 times that of the global LST, and the prominent increase in spring (0.068 ℃·a^{-1}) contributed the most to the overall warming. The LST is characterized by low

in the south and high in the north, and is signally influenced by the underlying surface characteristics such as elevation and vegetation coverage. The zonal decreasing law of temperature was broken by the distribution characteristics of gradually warming from south to north owing to the influence of altitude and the underlying surface, in which human activities play a paramount role in the process of LST change.

(3) HAI and LST were conspicuously positively correlated in the human activity area on the north slope of the Tianshan Mountains, and the overall distribution was strong in the east and weak in the west. The expression of its spatial differentiation and correlation were comprehensively affected by the range of human activities, manifestations, land-use changes, etc. Population distribution and nighttime light changes could support a rational explanation of LST changes. Human interventions related to vegetation such as agriculture and forestry planting and cultivation, urban greening and afforestation can effectively reduce the surface warming caused by human activities.

This study may not be able to fully incarnate the fluctuation period and the trend of longer time-series of geothermal change due to the time-series limitation of data such as nighttime light and population distribution, but the spatial correlation between LST and HAI is pronounced and objective, so it still has a relatively precise interpretation role for the assessment of the impact of human activities. In addition, this study mainly considered the direct disturbance of the ecosystem by human activities and fails to embody the indirect effects on the global scale, such as the long-distance diffusion and transmission of atmospheric pollutants, and the promotion of global base temperature caused by carbon emissions (not directly caused by local regions), etc. Furthermore, the introduction of big data such as pollutant concentration, traffic travel, points of interest, social media and so on should be capable of improving the characterization method of HAI more extensively, meticulously and multi-dimensionally, which needs to be further discussed in prospective research.

References

Chen Y B, Zheng Z H, Wu Z F *et al*., 2019. Review and prospect of application of nighttime light remote sensing data. *Progress in Geography*, 38(2): 205–223. (in Chinese)

Christelle V, Pietro C, Tufa D *et al*., 2009. Evaluation of MODIS land surface temperature data to estimate air temperature in different ecosystems over Africa. *Remote Sensing of Environment*, 114(2): 449–465.

Chu L X, 2019. Anthropogenic influence on coastal environment using satellite cloud-based platform [D]. Beijing: China University of Geosciences (Beijing). (in Chinese)

Cui Y X, 1998. Discussion on the causes, distribution and reconstruction and utilization of unused land in Liaoning province. *Chinese Land Science*, 12(2): 12–14. (in Chinese)

Deng Y H, Wang S J, Bai X Y *et al*., 2018. Relationship among land surface temperature and LUCC, NDVI in typical karst area. *Scientific Reports*, 8(1): 641–653.

Dong L P, 2012. Estimation of surface air temperature from MODIS land surface temperature and its application to the study of urban heat island in the East China Metropolitan Area [D]. Nanjing: Nanjing University of Information Science & Technology. (in Chinese)

Duan Q T, Luo L H, 2020. A dataset of human footprint over the Qinghai-Tibet Plateau during 1990–2015. *China Scientific Data*, 5(3): 303–312. (in Chinese)

Foster J L, 1983. Observations of the earth using nighttime visible imagery. *Proceedings of SPIE*: *The Interna-*

tional Society for Optical Engineering, 414(6): 187.

Guan Y L, Wang R H, Li C *et al*., 2015a. Spatial-temporal characteristics of land surface temperature in Tianshan Mountains area based on MODIS data. *Chinese Journal of Applied Ecology*, 26(3): 681–688. (in Chinese)

Guan Y L, Wang R H, Li C *et al*., 2015b. Variation characteristics of ground surface temperature in northern piedmont of Tianshan Mountains during 1963–2010. *Journal of Arid Meteorology*, 33(4): 587–594. (in Chinese)

Guo H L, Feng Z Z, He X H *et al*., 2019. The impact of surface cover and population density on urban land surface temperature: A case study of Zhengzhou city. *Journal of Inner Mongolia Normal University* (*Nature Science Edition*), 48(4): 298–306. (in Chinese)

Han M, Zhang C, Lu G *et al*., 2017. Response of wetland landscape pattern gradient to human activity intensity in Yellow River Delta. *Transactions of the Chinese Society of Agricultural Engineering*, 33(6): 265–274. (in Chinese)

He C Y, Shi P J, Li J G *et al*., 2006. Restoring urbanization process in China in the 1990s by using non-radiance-calibrated DMSP/OLS nighttime light imagery and statistical data. *Chinese Science Bulletin*, 51(13): 1614–1620.

Hu L F, Xie Y L, Cui S Y *et al*., 2021. The characteristics and driving forces of summer urban heat island in Guanzhong Plain urban agglomeration. *China Environmental Science*, 41(8): 3842–3852. (in Chinese)

Hu Y F, Zhao G H, Zhang Q L, 2018. Spatial distribution of population data based on nighttime light and LUC data in the Sichuan-Chongqing region. *Journal of Geo-information Science*, 20(1): 68–78. (in Chinese)

Huang F F, Ma W Q, Li M S *et al*., 2016. Analysis on responses of land surface temperature on the northern Tibetan Plateau to climate change. *Plateau Meteorology*, 35(1): 55–63. (in Chinese)

Li S C, Zhang X Z, 2018. Land use-based human activity intensity along the Yangtze River Economic Belt, China (1970s–2015). *China Scientific Data*, 3(3): 15–22. (in Chinese)

Li X, Li D R, Xu H M *et al*., 2017. Intercalibration between DMSP/OLS and VIIRS night-time light images to evaluate city light dynamics of Syria's major human settlement during Syrian Civil War. *International Journal of Remote Sensing*, 38(21): 5934–5951.

Liu C, Yan X Y, Jiang F Q, 2020a. Influence of precipitation distribution on desert vegetation of northern piedmont, Tianshan Mountains: Analysis based on daily NDVI and precipitation data. *Acta Ecologica Sinica*, 40(21): 7790–7804. (in Chinese)

Liu C, Zhang H Y, Li Q, 2020b. Spatiotemporal characteristics of human activity intensity and its driving mechanism in Hainan province from 1980 to 2018. *Progress in Geography*, 39(4): 567–576. (in Chinese)

Liu S L, Liu L M, Wu X *et al*., 2018. Quantitative evaluation of human activity intensity on the regional ecological impact studies. *Acta Ecologica Sinica*, 38(19): 6797–6809. (in Chinese)

Liu Z F, He C Y, Zhang Q F *et al*., 2012. Extracting the dynamics of urban expansion in China using DMSP-OLS nighttime light data from 1992 to 2008. *Landscape and Urban Planning*, 106(1): 62–72.

Lu Y, Yu W B, Guo M *et al*., 2017. Spatiotemporal variation characteristics of land cover and land surface temperature in Mohe County, Heilongjiang province. *Journal of Glaciology and Geocryology*, 39(5): 1137–1149. (in Chinese)

Luo G P, Chen X, Hu R J, 2003. Vegetation change during the last 10 years derived from satellite image in the north slopes of the Tianshan Mountains. *Journal of Glaciology and Geocryology*, 25(2): 237–242. (in Chinese)

Ma T, Zhou Y K, Zhou C H *et al*., 2015. Night-time light derived estimation of spatio-temporal characteristics of urbanization dynamics using DMSP/OLS satellite data. *Remote Sensing of Environment*, 158: 453–464.

Mao W Y, Chen Y, Cao X, 2016. Evaluation index of cold wave intensity at a single station and its application in

Urumqi. *Journal of Meteorology and Environment*, 32(5): 139–146. (in Chinese)

Marc L I, Ping Z, Robert E W *et al*., 2009. Remote sensing of the urban heat island effect across biomes in the continental USA. *Remote Sensing of Environment*, 114(3): 504–513.

Ouyang B, Che T, Dai L Y *et al*., 2012. Estimating mean daily surface temperature over the Tibetan Plateau based on MODIS LST products. *Journal of Glaciology and Geocryology*, 34(2): 296–303. (in Chinese)

Pan J H, Li J F, 2016. Estimate and spatio-temporal dynamics of electricity consumption in China based on DMSP/OLS images. *Geographical Research*, 35(4): 627–638. (in Chinese)

Prihodko L, Goward S N, 1997. Estimation of air temperature from remotely sensed surface observations. *Remote Sensing of Environment*, 60(3): 335–346.

Qi Y X, Zhang F, Chen R *et al*., 2020. Vegetation coverage dynamics in northern slope of Tianshan Mountains from 2001 to 2015. *Acta Ecologica Sinica*, 40(11): 3677–3687. (in Chinese)

Qiao Z, Huang N Y, Xu X L *et al*., 2019. Spatio-temporal pattern and evolution of the urban thermal landscape in metropolitan Beijing between 2003 and 2017. *Acta Geographica Sinica*, 74(3): 475–489. (in Chinese)

Reyilai K, Yusupujiang R, Gao Q *et al*., 2016. Spatiotemporal response of land surface temperature to land use/cover change in Yanqi Basin, Xinjiang. *Transactions of the Chinese Society of Agricultural Engineering*, 32(20): 259–266. (in Chinese)

Rong Y, Li C, Xu C *et al*., 2017. Ecosystem service values and spatial differentiation changes during urbanization: A case study of Huanghua city. *Chinese Journal of Ecology*, 36(5): 1374–1381. (in Chinese)

Sanderson E W, Jaiteh M, Levy M A *et al*., 2002. The human footprint and the last of the wild. *Bioscience*, 52(10): 891–904.

Shen Y P, Wang G Y, 2013. Key findings and assessment results of IPCC WGI Fifth Assessment Report. *Journal of Glaciology and Geocryology*, 35(5): 1068–1076. (in Chinese)

Shen Z J, Zeng J, 2021. Spatial relationship of urban development to land surface temperature in three cities of southern Fujian. *Acta Geographica Sinica*, 76(3): 566–583. (in Chinese)

Shi Y F, Shen Y P, Hu R J, 2002. Preliminary study on signal, impact and foregorund of climatic shift from warmdry to warm-humid in northwest China. *Journal of Glaciology and Geocryology*, 24(3): 219–226. (in Chinese)

Shi Y F, Shen Y P, Li D L *et al*., 2003. Discussion on the characteristics and trend of climate transition from warm and wet in western China. *Quaternary Science*, 23(2): 152–164. (in Chinese)

Sun Q M, Liu T, Han Z Q *et al*., 2014. Response of climate changes on vegetation cover in north of Tianshan Mountains evaluates using multiple time scales. *Transactions of the Chinese Society of Agricultural Engineering* (*Transactions of the CSAE*), 30(15): 248–255. (in Chinese)

Venter O, Sanderson E W, Magrach A *et al*., 2016a. Global terrestrial human footprint maps for 1993 and 2009. *Scientific Data*, 3(1780): 160067.

Venter O, Sanderson E W, Magrach A *et al*., 2016b. Sixteen years of change in the global terrestrial human footprint and implications for biodiversity conservation. *Nature Communications*, 7(1): 12558.

Wang G, Zhang Q P, Xiao R B *et al*., 2019. On impacts of land use, population density and altitude on the urban heat island. *Journal of Yunnan University* (*Natural Sciences Edition*), 41(1): 82–90. (in Chinese)

Wang H R, Zheng X Q, Yuan T, 2012. Overview of researches based on DMSP/OLS nighttime light data. *Progress in Geography*, 31(1): 11–19. (in Chinese)

Wang J S, 2008. Study on the spatial characteristic of land surface temperature and the relationship between the spatial characteristic of land surface temperature and land surface characteristic in Beijing area [D]. Shijiazhuang: Hebei Normal University. (in Chinese)

Wang L J, Li J L, Tian P *et al*., 2020. Impacts of human activity on coastal wetland land cover changes related to reclamation on the south coast of Hangzhou Bay. *Shanghai Land & Resources*, 41(1): 4–10. (in Chinese)

Wang P Y, Li Z Q, Li H L *et al*., 2017. Analysis of the relation between glacier volume change and area change in the Tianshan Mountains. *Journal of Glaciology and Geocryology*, 39(1): 9–15. (in Chinese)

Wei F Y, 2007. Statistic Diagnostic and Forecast Technologies in Climatology. Beijing: China Meteorological Press. (in Chinese)

Xia J S, Du P J, Zhang H R *et al*., 2010. The quantitative relationship between land surface temperature and land cover types based on remotely sensed data. *Remote Sensing Technology and Application*, 25(1): 15–23. (in Chinese)

Xu Y, Xu X R, Tang Q, 2016. Human activity intensity of land surface: Concept, methods and application in China. *Journal of Geographical Sciences*, 26(9): 1349–1361.

Xue C L, Zhang H Q, Zhou Tao *et al*., 2021. Ecological quality and its relationships with human activities in China-Laos railway economic belt. *Chinese Journal of Applied Ecology*, 32(2): 638–648. (in Chinese)

Yang G J, Sun C H, Li H, 2015. Verification of high-resolution land surface temperature by blending ASTER and MODIS data in Heihe River Basin. *Transactions of the Chinese Society of Agricultural Engineering*, 31(6): 193–200. (in Chinese)

Yang R F, 2018. Integrating DMSP/OLS & NPP/VIIRS nighttime light data to the application research of urban agglomeration growth process [D]. Chongqing: Southwest University. (in Chinese)

Yin X J, Zhu H H, Gao J *et al*., 2020. Effects of climate change and human activities on net primary productivity in the northern slope of Tianshan, Xinjiang, China. *Transactions of the Chinese Society of Agricultural Engineering*, 36(20): 195–202. (in Chinese)

Yun X, 2019. Improvement of surface temperature and warming analysis [D]. Beijing: China Meteorological Science Research Institute. (in Chinese)

Zeng J, 2015. Remote sensing monitoring of land use change Impacts on land surface temperature [D]. Guilin: Guangxi Normal University. (in Chinese)

Zhang C Y, Wang Z, 2004. Quantitative assessment of human activity intensity in the Heihe catchment. *Advance in Earth Sciences*, 19(Supp1.1): 386–390. (in Chinese)

Zhang J H, Hou Y L, Li G C *et al*., 2005. Satellite remote sensing research and impact factor analysis of diurnal variation and seasonal characteristics of heat island in Beijing and its surrounding areas. *Science in China*: *Series D*, 35(Suppl.1): 187–194. (in Chinese)

Zhang Q L, Schaaf C, Seto K C, 2013. The vegetation adjusted NTL urban index: A new approach to reduce saturation and increase variation in nighttime luminosity. *Remote Sensing of Environment*, 129(2): 32–41.

Zhang Y N, Pan J H, 2019. Spatio-temporal simulation and differentiation pattern of carbon emissions in China based on DMSP/OLS nighttime light data. *China Environmental Science*, 39(4): 1436–1446. (in Chinese)

Zhang Z Y, Liu L, He X L *et al*., 2019. Evaluation on glaciers ecological services value in the Tianshan Mountains, Northwest China. *Journal of Geographical Sciences*, 29(1): 101–114.

Zhao G S, Liu J Y, Kuang W H *et al*., 2015. Disturbance impacts of land use change on biodiversity conservation priority areas across China: 1990–2010. *Journal of Geographical Sciences*, 25(5): 515–529.

Zhong C X, Zhou Y Z, 2008. Population distribution and regional economic development in economic belt at north slope of Tianshan. *Journal of Arid Land Resources and Environment*, (6): 33–38. (in Chinese)